ARTICLE IN PRESS
JID:AESCTE AID:106843 /FLA [m5G; v1.307] P.1 (1-10)
Aerospace Science and Technology ••• (••••) ••••••

Contents lists available at ScienceDirect

Aerospace Science and Technology

www.elsevier.com/locate/aescte

Continuum deformation of a multi-quadcopter system under a time-varying communication weights

Hossein Rastgoftar [a,*], Sergey Nersesov [b]

[a] Aerospace and Mechanical Engineering Department, University of Arizona, Tucson, AZ, USA
[b] Mechanical Engineering Department, Villanova University, Villanova, PA, USA

ARTICLE INFO

Article history:
Received 5 September 2020
Received in revised form 12 February 2021
Accepted 17 May 2021
Available online xxxx
Communicated by Efstathios Bakolas

Keywords:
Multi-agent coordination
Local communication
Leader-follower
Unmanned vehicles
Collision avoidance

ABSTRACT

This paper studies the problem of continuum deformation of a multi-quadcopter system (MQS) under time-varying communication weights. Quadcopters are treated as particles of a deformable body with time-varying parameters, where a desired n-D continuum deformation is planned based on the trajectories of $n+1$ leaders placed at the vertices of n-D simplex. The followers distributed inside the simplex acquire the desired continuum deformation by local communication with time varying communication weights, where stability and convergence of the MQS continuum deformation can be proven. This paper formally characterizes safety of the MQS continuum deformation by ensuring inter agent collision avoidance and follower containment. Therefore, a large-scale MQS can safely deform in an obstacle-laden environment with modest computational cost.

1. Introduction

Multi-agent coordination has been an active research area and has found many applications such as surveillance [1,2], formation flight [3,4], traffic coordination and control [5], rescue missions [6], and cooperative payload transport [7,8]. Cooperative control and group coordination offer robustness and resilience to failure and reduces mission cost.

1.1. Related work

So far researchers have proposed a variety of centralized and decentralized multi-agent coordination approaches such as Virtual Structure [9], Consensus [10–16], and Containment Control [17–22]. Virtual Structure is a centralized coordination approach treating agents as particles of a virtual rigid body. Consensus is the most common decentralized coordination approach that has been extensively studied by the researchers in the past two decades. Leader-less [11,23] and leader-follower consensus [10,24], retarded consensus coordination [14,16], and consensus under fixed and switching communication topologies [15] have been intensively studied in the past. Containment control is a leader-follower approach in which leaders guide the bulk motion and followers acquire the desired coordination in a decentralized fashion through local communication. Stability and convergence of containment control coordination have been studied in [17,18]. Also, containment control in the presence of communication delay was presented in [20,21,25]. Leader-follower containment under switching communication topology is shown in [22]. Finite-time containment is investigated in [26,27].

Continuum deformation of multi-agent systems is a recent approach that treats agents/vehicles and particles of a deformable body. Similar to containment control, continuum deformation is a leader-follower approach; the bulk motion is guided by leaders and followers acquire the desired coordination through local communication in real time. However, continuum deformation characterizes safety and provides characteristic equations for the followers communication weights. In particular, collision avoidance and follower containment are guaranteed in a large-scale continuum deformation coordination while the multi agent system can aggressively deform in an obstacle-laden environment.

1.2. Contribution

Although existing continuum deformation allows aggressive deformation for group coordination in a cluttered environment, followers' communication weights are restricted to be fixed and are determined based on the initial formation of the agents [7,28]. This will result in a so-called "deformable rigidity" limitation and limit maneuverability of the group coordination. This paper deals with the "deformable rigidity" problem by advancing the existing

* Corresponding author.
E-mail addresses: hrastgoftar@arizona.edu (H. Rastgoftar), sergey.nersesov@villanova.edu (S. Nersesov).

https://doi.org/10.1016/j.ast.2021.106843
1270-9638/

Please cite this article as: H. Rastgoftar and S. Nersesov, Continuum deformation of a multi-quadcopter system under a time-varying communication weights, Aerospace Science and Technology, https://doi.org/10.1016/j.ast.2021.106843

continuum deformation coordination approach towards continuum deformation of multi-vehicle system under a time-varying communication protocol. In particular, we treat a quadcopter team as particles of a deformable body with time-varying material properties. By classifying quadcopters as leaders and followers, leaders' coordination is defined by an affine transformation while followers acquire the desired coordination through local communication. As the first contribution of the paper, we will prove stability and convergence of the quadcopter coordination defined by an affine transformation with time-varying communication weights. Specifically, we prove that the transient error characterizing deviation form the global desired trajectory is bounded for every quadcopter i. The second contribution of this paper is to specify and verify safety in a decentralized continuum deformation coordination with time-varying communication. Therefore, a large number of agents can significantly deform in a geometrically constrained environment while guaranteeing collision avoidance.

The proposed decentralized time-varying MQS continuum deformation can be potentially used for cooperative aerial payload transport applications in which a quadcopter team robustly carry a heavy payload in a geometrically-constrained environment. The interest in using multi-copters for aerial payload transport and package delivery applications [7] has been grown over the past few years. Big companies such as Amazon, Google, and UPS have already tested and commercialized safe package delivery missions using drones. In spite of the huge interest for aerial payload transport, delivery drone operations are limited to carrying light payloads. By relaxing the so-called "deformable rigidity" of the existing continuum deformation coordination, the MQS can aggressively deform to pass through narrow channels while the proposed time-varying communication topology enables them to effectively provide proper stability forces through optimizing the spatial distribution of the follower quadcopters.

This paper is organized as follows. Preliminary notions provided in Section 2 are followed by Problem Formulation in Section 3. Decentralized coordination of the quadcopter team as well as multi-quadcopter system (MQS) dynamics and control are presented in Sections 4 and 5, respectively. Safety of the MQS coordination is mathematically characterized in Section 7. Simulation results presented in Section 8 are followed by Conclusion in Section 9.

2. Preliminaries

2.1. Graph theory notions

Consider a multi-quadcopter system (MQS) consisting of N agents where every agent is identified by a unique index number defined by set $\mathcal{V}$. Inter-agent communication is defined by connected graph $\mathcal{G}(\mathcal{V},\mathcal{E})$ with node set $\mathcal{V}$ and edge set $\mathcal{E}\subset\mathcal{V}\times\mathcal{V}$. Agents are treated as particles of an n-D deformable body ($n=2,3$), where the desired coordination is defined by $n+1$ leaders identified by set $\mathcal{V}_L=\{1,\cdots,n+1\}$. The remaining agents are identified by set $\mathcal{V}_F=\mathcal{V}\setminus\mathcal{V}_L$ representing followers. In-neighbor set $\mathcal{N}_i$ of vehicle $i\in\mathcal{V}$ is defined by set $\{j\big|(j,i)\in\mathcal{E}\}$; follower $i\in\mathcal{V}$ has access to the position information of in-neighbor $j\in\mathcal{N}_i$ at any time t. Because leaders move independently, they do not rely on followers' position information, thus, $\mathcal{N}_i=\emptyset$, if $i\in\mathcal{V}_L$.

Assumption 1. In this paper, graph $\mathcal{G}$ is defined such that the following properties hold:

1. Follower-follower communication is bidirectional which implies that, for $i,j\in\mathcal{V}_F$, if $(j,i)\in\mathcal{E}$, then $(i,j)\in\mathcal{E}$.
2. Leader-follower communication is unidirectional which implies that, for $j\in\mathcal{V}_L$ and $i\in\mathcal{V}_F$, if $(j,i)\in\mathcal{E}$, then $(i,j)\notin\mathcal{E}$.
3. Position information of leader $j\in\mathcal{V}_L$ is communicated to only one follower agent $i\in\mathcal{V}_F$.

2.2. Motion space discretization

Let $\mathbf{p}_1\in\mathbb{R}^n$, $\mathbf{p}_2\in\mathbb{R}^n$, $\cdots$, $\mathbf{p}_{n+1}\in\mathbb{R}^n$ and $\mathbf{c}\in\mathbb{R}^n$ define $n+2$ points in $\mathbb{R}^n$. We define rank operator

$$\rho\left(\mathbf{p}_1,\cdots,\mathbf{p}_{n+1}\right)=\mathrm{rank}\left(\begin{bmatrix}\mathbf{p}_2-\mathbf{p}_1 & \cdots & \mathbf{p}_{n+1}-\mathbf{p}_1\end{bmatrix}\right). \tag{1}$$

Note that $0\le\rho\left(\mathbf{p}_1,\cdots,\mathbf{p}_{n+1}\right)\le n$. If $\rho\left(\mathbf{p}_1,\cdots,\mathbf{p}_{n+1}\right)=n$, $\mathbf{p}_1$, $\mathbf{p}_2$, $\cdots$, $\mathbf{p}_{n+1}$ determine positions of vertices of an n-D simplex and we can define operator $\mathbf{\Omega}\left(\mathbf{p}_1,\cdots,\mathbf{p}_{n+1},\mathbf{c}\right)$ as follows:

$$\mathbf{\Omega}\left(\mathbf{p}_1,\cdots,\mathbf{p}_{n+1},\mathbf{c}\right)=\begin{bmatrix}\mathbf{p}_1 & \cdots & \mathbf{p}_{n+1}\\ 1 & \cdots & 1\end{bmatrix}^{-1}\begin{bmatrix}\mathbf{c}\\ 1\end{bmatrix}\in\mathbb{R}^{(n+1)\times 1} \tag{2}$$

It was shown in [28] that if each element of the vector $\mathbf{\Omega}(\mathbf{p}_1,\cdots,\mathbf{p}_{n+1},\mathbf{c})$ is nonnegative, then $\mathbf{c}$ is inside the simplex formed by vectors $\mathbf{p}_1$, $\mathbf{p}_2$, $\cdots$, $\mathbf{p}_{n+1}$. Otherwise $\mathbf{c}$ is outside the simplex. It was also shown in [28] that the sum of elements of $\mathbf{\Omega}\left(\mathbf{p}_1,\cdots,\mathbf{p}_{n+1},\mathbf{c}\right)$ is 1.

2.3. Position notations

Without loss of generality, in this paper we consider teams of quadcopters coordinating in a 3-D motion space where quadcopters are treated as particles of an n-D continuum, where $n\in\{1,2,3\}$. Throughout this paper, we use the following notation.

Actual Position: Actual position of vehicle $i\in\mathcal{V}$ is denoted by $\mathbf{r}_i[k]=[x_i[k]\ y_i[k]\ z_i[k]]^T$ and is considered as the output of the control system of each vehicle.

Global Desired Position: Global desired position of vehicle $i\in\mathcal{V}$ is given by

$$\mathbf{r}_{i,HT}\left[k\right]=\begin{cases}\mathbf{Q}\left[k\right]\mathbf{r}_{i,0}+\mathbf{d}\left[k\right] & i\in\mathcal{V}_L\\ \sum_{j\in\mathcal{V}_L}^{n+1}\alpha_{i,j}[k]\mathbf{r}_j\left[k\right] & i\in\mathcal{V}_F\end{cases},\qquad k=0,1,\cdots, \tag{3}$$

where $\mathbf{Q}[k]\in\mathbb{R}^{3\times 3}$ is the Jacobian nonsingular matrix for each $k\ge 0$ characterizing the deformation of the singleton formed by the leader vehicles $i\in\mathcal{V}_L$. Also, $\mathbf{d}[k]$ is the rigid-body displacement vector characterizing the displacement of the above singleton and $\mathbf{r}_{i,0}=\begin{bmatrix}x_{i,0} & y_{i,0} & z_{i,0}\end{bmatrix}^T$ is the material coordinate of follower vehicle $i\in\mathcal{V}_F$. Note that the material coordinate is constant. Furthermore,

$$\begin{bmatrix}\alpha_{i,1}[k]\\ \vdots\\ \alpha_{i,n+1}[k]\end{bmatrix}=\mathbf{\Omega}\left(\mathbf{r}_{1,HT},\cdots,\mathbf{r}_{n+1,HT},\mathbf{r}_{i,HT}\right),\qquad\forall i\in\mathcal{V}_F, \tag{4}$$

where parameters $\alpha_{i,1}[k]\ \cdots\ \alpha_{i,n+1}[k]$ sum up to 1 at every instant of time k, that is,

$$\sum_{j\in\mathcal{V}_L}\alpha_{i,j}[k]=1\qquad k=0,1,\cdots. \tag{5}$$

Local Desired Position: Local desired position is given by

$$\begin{cases}\mathbf{r}_{i,d}\left[k\right]=\mathbf{r}_{i,HT}\left[k\right] & i\in\mathcal{V}_L\\ \mathbf{r}_{i,d}\left[k\right]=\sum_{j\in\mathcal{N}_i}w_{i,j}[k]\mathbf{r}_j[k] & i\in\mathcal{V}_F\end{cases},\qquad k=0,1,\cdots. \tag{6}$$

Note that local desired position of follower $i\in\mathcal{V}_F$ is defined as the convex combination of the positions of its in-neighbors, where $w_{i,j}[k]$ is the communication weight of agent $j\in\mathcal{N}_i$ with agent $i\in\mathcal{V}$ at discrete time k.

3. Problem formulation

Consider a MQS consisting of N quadcopters, where dynamics of quadcopter $i \in \mathcal{V}$ are given by

$$\begin{cases} \mathbf{x}_i[k+1] = \mathbf{f}_i\left[\mathbf{x}_i[k]\right] + \mathbf{g}_i\left[\mathbf{x}_i[k]\right]\mathbf{u}_i[k] \\ \mathbf{r}_i[k] = \left[x_i[k]\ y_i[k]\ z_i[k]\right]^T \end{cases}, \tag{7}$$

$\mathbf{f}_i$ and $\mathbf{g}_i$ are smooth functions, and $\mathbf{x}_i$, $\mathbf{u}_i$, and $\mathbf{r}_i$ denote state, input, and output vectors, respectively, i.e. actual position of quadcopter $i \in \mathcal{V}$ is considered as the output vector. Every quadcopter i applies a feedback linearization control to track the local desired trajectory defined by (6). This ensures that the global desired trajectory, defined by affine transformation (3), is acquired in a decentralized fashion via local communication.

The first objective of the paper is to guarantee the stability and convergence of decentralized continuum deformation coordination of the quadcopter team, that is, to guarantee the convergence of the actual position $\mathbf{r}_i$ to the global desired position for each quadcopter in the network, where inter-agent communications are time-varying and weighted. Defining safety box

$$\begin{aligned} \forall k, \qquad \mathcal{B}_i[k] = \{(x\ y\ z) \mid & \left|x[k] - x_{i,HT}[k]\right| \le \delta, \\ & \left|y[k] - y_{i,HT}[k]\right| \le \delta,\ \left|z[k] - z_{i,HT}[k]\right| \le \delta\}. \end{aligned} \tag{8}$$

Each quadcopter $i \in \mathcal{V}$ must be inside the safety box at every discrete time k:

$$\forall k, \qquad \mathbf{r}_i[k] \in \mathcal{B}_i \tag{9}$$

where the vertices of the safety box $\mathcal{B}_i$ are defined by the set of points

$$\begin{aligned} \mathcal{I}\left(\mathbf{r}_{i,HT}\right) = \Bigg\{ & \underbrace{\begin{bmatrix} x_{i,HT}+\delta \\ y_{i,HT}+\delta \\ z_{i,HT}+\delta \end{bmatrix}}_{\mathbf{b}_{i,1}}, \underbrace{\begin{bmatrix} x_{i,HT}+\delta \\ y_{i,HT}+\delta \\ z_{i,HT}-\delta \end{bmatrix}}_{\mathbf{b}_{i,2}}, \underbrace{\begin{bmatrix} x_{i,HT}+\delta \\ y_{i,HT}-\delta \\ z_{i,HT}+\delta \end{bmatrix}}_{\mathbf{b}_{i,3}}, \\ & \underbrace{\begin{bmatrix} x_{i,HT}+\delta \\ y_{i,HT}-\delta \\ z_{i,HT}-\delta \end{bmatrix}}_{\mathbf{b}_{i,4}}, \underbrace{\begin{bmatrix} x_{i,HT}-\delta \\ y_{i,HT}+\delta \\ z_{i,HT}+\delta \end{bmatrix}}_{\mathbf{b}_{i,5}}, \underbrace{\begin{bmatrix} x_{i,HT}-\delta \\ y_{i,HT}+\delta \\ z_{i,HT}-\delta \end{bmatrix}}_{\mathbf{b}_{i,6}}, \\ & \underbrace{\begin{bmatrix} x_{i,HT}-\delta \\ y_{i,HT}-\delta \\ z_{i,HT}+\delta \end{bmatrix}}_{\mathbf{b}_{i,7}}, \underbrace{\begin{bmatrix} x_{i,HT}-\delta \\ y_{i,HT}-\delta \\ z_{i,HT}-\delta \end{bmatrix}}_{\mathbf{b}_{i,8}} \Bigg\} \end{aligned} \tag{10}$$

Note that $\mathcal{I}\left(\mathbf{r}_{i,HT}\right) = \left\{\mathbf{b}_{i,1}, \cdots, \mathbf{b}_{i,8}\right\}$ where $i \in \mathcal{V}_L$ and $\mathbf{b}_{i,j}$ is the j-th member of $\mathcal{I}\left(\mathbf{r}_{i,HT}\right)$, i.e. $j = 1, \cdots, 8$.

The second objective of the paper is to formally specify and verify inter-agent collision avoidance at every discrete time k. Assuming every quadcopter is enclosed by a ball of radius $\epsilon \ge 0$, inter-agent collision avoidance is guaranteed, if

$$\|\mathbf{r}_i[k] - \mathbf{r}_j[k]\| \ge 2\epsilon, \quad k \ge 0, \quad i, j \in \mathcal{V}, i \ne j. \tag{11}$$

The third objective of the paper is to ensure that no follower quadcopter leaves the leading simplex defined by leaders 1 through $n+1$. To this end, we define

$$\mathcal{S}[k] = \mathcal{I}\left(\mathbf{r}_{1,HT}[k]\right) \times \cdots \times \mathcal{I}\left(\mathbf{r}_{n+1,HT}[k]\right), \quad k \ge 0,$$

as the set of all n-D simplexes made by vertices of $n+1$ safety boxes surrounding leaders 1 through $n+1$ at discrete time k, where $\times$ is the Cartesian product symbol. Expressing $\mathcal{S}$ by

$$\mathcal{S}[k] = \underbrace{\bigwedge_{j_1=1}^{8} \cdots \bigwedge_{j_{n+1}=1}^{8}}_{\text{n+1 } times} \left(\mathbf{b}_{1,j_1}, \cdots, \mathbf{b}_{n+1,j_{n+1}}\right), \quad k \ge 0, \tag{12}$$

follower containment condition is specified as follows:

$$\begin{aligned} & \bigwedge_{i \in \mathcal{V}_F} \underbrace{\bigwedge_{j_1=1}^{8} \cdots \bigwedge_{j_{n+1}=1}^{8}}_{\text{n+1 } times} \\ & \times \bigwedge_{\left(\mathbf{b}_{1,j}[k], \cdots, \mathbf{b}_{n+1,j}[k]\right) \in \mathcal{S}} \boldsymbol{\Omega}\left(\mathbf{b}_{1,j_1}[k], \cdots, \mathbf{b}_{n+1,j_{n+1}}[k], \mathbf{r}_i[k]\right) \ge 0, \end{aligned} \tag{13}$$

at every discrete time k where $\mathbf{b}_{l,j_l} \in \mathcal{I}\left(\mathbf{r}_{l,HT}\right)$ is the desired position of vertex $j_l \in \{1, \cdots, 8\}$ of the safety box enclosing $\mathbf{r}_{l,HT}$ ($l \in \mathcal{V}_L$), and $\mathbf{r}_i[k]$ denote the actual position of follower $i \in \mathcal{V}_F$ at discrete time k.

4. Communication topology

In this paper, the inter-agent communications among quadcopters are weighted and defined by a time-varying set

$$\mathcal{W}[k] = \left\{ w_{i,j}[k] \in [0,1] : (j,i) \in \mathcal{E}, \sum_{j \in \mathcal{N}_i} w_{i,j}[k] = 1,\ k \in \mathbb{N} \right\}. \tag{14}$$

Assumption 2. It is assumed that in-neighbor set $\mathcal{N}_i$ is fixed although communication weight $w_{i,j}[k]$ is time-varying.

Given set $\mathcal{W}$, we can define matrix $\mathbf{W}[k] = \left[W_{ij}[k]\right] \in \mathbb{R}^{N \times N}$ with the ij entry

$$W_{ij}[k] = \begin{cases} w_{i,j}[k] & j \in \mathcal{N}_i \wedge i \in \mathcal{V}_F \\ 0 & \text{otherwise} \end{cases}. \tag{15}$$

Note that matrix $\mathbf{W}$ is one-sum row, i.e. sum of every row of matrix $\mathbf{W}$ is 1. Matrix $\mathbf{W}$ can be partitioned as

$$\mathbf{W}[k] = \begin{bmatrix} \mathbf{0} & \mathbf{0} \\ \mathbf{B}[k] & \mathbf{A}[k] \end{bmatrix}, \tag{16}$$

where $\mathbf{B} \in \mathbb{R}^{(N-n-1)\times(n+1)}$ and $\mathbf{A} \in \mathbb{R}^{(N-n-1)\times(N-n-1)}$. It was shown in [28] that $\mathbf{A}$ and $\mathbf{B}$ are nonnegative matrices (in a sense that each entry is nonnegative) with $\mathbf{A}$ having zero diagonal elements.

Remark 1. Per the third property of Assumption 1, every column of matrix $\mathbf{B} \in \mathbb{R}^{(N-n-1)\times(n+1)}$ has only one positive element.

Theorem 1. *Assume graph $\mathcal{G}(\mathcal{V}, \mathcal{E})$ is defined such that Assumption 1 is satisfied and communication weights are defined by $\mathcal{W}$. Then, matrix $\mathbf{A}[k]$ is irreducible [29] at every discrete time k and eigenvalues of matrix $\mathbf{A}[k]$ are contained inside an open unit disk centered at the origin. Furthermore, matrix*

$$\mathbf{W}_L[k] = \mathbf{D}^{-1}\mathbf{B}[k] \tag{17}$$

is non-negative and one-sum row at every discrete time k, where

$$\mathbf{D}[k] = -\mathbf{I} + \mathbf{A}[k]. \tag{18}$$

Proof. Because graph $\mathcal{G}$ satisfies Assumption 1, matrix $\mathbf{A}$ is irreducible. It follows from Assumption 1 and Remark 1 that $N-2(n+1)$ rows of matrix $\mathbf{A}$ sum up to 1, and the remaining rows all sum to a positive number less than 1. It follows from Perron-Frobenius theorem [29] that the spectral radius of matrix $\mathbf{A}$, denoted by r_A, is less than 1 which in turn implies that eigenvalues of $\mathbf{A}$ are all placed inside a disk of radius $r_A < 1$. This also implies that the eigenvalues of $\mathbf{D} = -\mathbf{I} + \mathbf{A}$ are contained inside an open unit disk centered at $-1 + 0j$. Therefore, $\mathbf{D}$ is invertible. Let $\mathbf{L} = [\mathbf{B}\ \mathbf{D}]$ and let $\tilde{\mathbf{L}} = \mathbf{D}^{-1}\mathbf{L} = [\mathbf{D}^{-1}\mathbf{B}\ \mathbf{I}]$. Note that since $[\mathbf{B}\ \mathbf{A}]$ is a one-sum row matrix, it follows that $\mathbf{L}$ is zero-sum row matrix. Furthermore, it can be seen from the definition of $\tilde{\mathbf{L}} = \mathbf{D}^{-1}\mathbf{L}$ and the fact that $\mathbf{L}$ is zero-sum-row that $\tilde{\mathbf{L}}$ is also a zero-sum row matrix. Consequently, sum of the row entries of matrix $\mathbf{W}_L = -\mathbf{D}^{-1}\mathbf{B}$ is 1. Furthermore, matrix $\mathbf{W}_L$ is non-negative. Indeed, it follows from the definition of $\mathbf{D}$ in (18) that its inverse can be written as

$$\mathbf{D}^{-1} = -\sum_{i=0}^{\infty} \mathbf{A}^i. \tag{19}$$

Hence,

$$\mathbf{W}_L = -\mathbf{D}^{-1}\mathbf{B} = \sum_{i=0}^{\infty} \mathbf{A}^i\mathbf{B}. \tag{20}$$

Since all elements of $\mathbf{A}$ and $\mathbf{B}$ are non-negative, it follows that the elements of $\mathbf{W}_L$ are also non-negative. $\square$

Stability and convergence of the network dynamics under time-varying communication weights was shown in [30]. The main focus of the current paper is to formally analyze safety of MQS continuum deformation coordination in an obstacle-laden environment.

Theorem 2. *Suppose graph $\mathcal{G}$ is defined such that Assumption 1 is satisfied and component of $q \in \{x, y, z\}$ of the global desired positions of followers can be related to the component $q \in \{x, y, z\}$ of the global desired positions of the leaders by*

$$\mathbf{z}_{q,F,HT} = \mathbf{W}_L \mathbf{z}_{q,L,HT}, \qquad q \in \{x, y, z\}, \tag{21}$$

where

$$\mathbf{W}_L[k] = \begin{bmatrix} \mathbf{\Omega}^T\left(\mathbf{r}_{1,HT}, \cdots, \mathbf{r}_{n+1,HT}, \mathbf{r}_{n+2,HT}\right) \\ \vdots \\ \mathbf{\Omega}^T\left(\mathbf{r}_{1,HT}, \cdots, \mathbf{r}_{n+1,HT}, \mathbf{r}_{N,HT}\right) \end{bmatrix} \in \mathbb{R}^{(N-n-1)\times(n+1)} \tag{22}$$

and

$$\mathbf{z}_{q,L,HT}[k] = \begin{bmatrix} q_{1,HT}[k] & \cdots & q_{n+1,HT}[k] \end{bmatrix}^T \in \mathbb{R}^{(n+1)\times 1}, \quad q \in \{x, y, z\}, \tag{23a}$$

$$\mathbf{z}_{q,F,HT}[k] = \begin{bmatrix} q_{n+2,HT}[k] & \cdots & q_{N,HT}[k] \end{bmatrix}^T \in \mathbb{R}^{(N-n-1)\times 1}, \quad q \in \{x, y, z\}, \tag{23b}$$

define position components of the leaders and followers, respectively.

Proof. If $\delta = 0$, then, actual, local desired, and global desired positions of every quadcopter $i \in \mathcal{V}$ are the same, and we can write

$$\begin{cases} \bigwedge_{i\in\mathcal{V}_L}\left(\mathbf{r}_{i,HT}[k] - \mathbf{r}_{i,d}[k] = \mathbf{0}\right) \\ \bigwedge_{i\in\mathcal{V}_F}\left(\mathbf{r}_{i,HT}[k] - \sum_{j\in\mathcal{N}_i} w_{i,j}[k]\mathbf{r}_{j,HT}[k] = \mathbf{0}\right) \end{cases} \tag{24}$$

at every discrete time k. If Eq. (24) is satisfied, then, we can write

$$\mathbf{z}_{q,F,HT}[k] = \mathbf{A}\mathbf{z}_{q,F,HT}[k] + \mathbf{B}\mathbf{z}_{q,L,HT}[k] \tag{25}$$

at every discrete time k, which in turn implies that

$$\mathbf{z}_{q,F,HT} = -\left(-\mathbf{I} + \mathbf{A}\right)^{-1}\mathbf{B}\mathbf{z}_{q,L,HT} = -\mathbf{D}^{-1}\mathbf{B}\mathbf{z}_{q,L,HT} = \mathbf{W}_L\mathbf{z}_{q,L,HT},$$

where $\mathbf{A}$ and $\mathbf{B}$ are defined in (16), $\mathbf{W}_L$ is non-negative and one-sum-row per Theorem 1. Therefore, row i of Eq. (21) gives the component $q \in \{x, y, z\}$ of the global desired position of follower $(i+n+1) \in \mathcal{V}_F$ expressed with respect to the leaders, where row i of matrix $\mathbf{W}_L$ is the same as Eq. (4). $\square$

5. Quadcopter dynamics

We say that

$$\mathbf{r}_i[k] = [x_i[k]\ y_i[k]\ z_i[k]]^T,$$
$$\mathbf{v}_i[k] = \left[v_{x,i}[k]\ v_{y,i}[k]\ v_{z,i}[k]\right]^T,$$
$$\mathbf{a}_i[k] = \left[a_{x,i}[k]\ a_{y,i}[k]\ a_{z,i}[k]\right]^T,$$
$$\mathbf{J}_i[k] = \left[J_{x,i}[k]\ J_{y,i}[k]\ J_{z,i}[k]\right]^T$$

denote position, velocity, acceleration, and jerk of quadcopter $i \in \mathcal{V}$ at discrete time k. Quadcopter i's body axes are denoted by $\hat{\mathbf{i}}_{b,i}$, $\hat{\mathbf{j}}_{b,i}$, and $\hat{\mathbf{k}}_{b,i}$, and $\hat{\mathbf{e}}_x = [1\ 0\ 0]^T$, $\hat{\mathbf{e}}_y = [0\ 1\ 0]^T$, and $\hat{\mathbf{e}}_z = [0\ 0\ 1]^T$ are the base vectors of the inertial (Cartesian) coordinate system. Body axes of quadcopter $i \in \mathcal{V}_F$ are related to the base vectors of the inertial coordinate system via Euler angles as follows

$$\begin{bmatrix} \hat{\mathbf{i}}_{b,i} \\ \hat{\mathbf{j}}_{b,i} \\ \hat{\mathbf{k}}_{b,i} \end{bmatrix} = \mathbf{R}\left(\phi_i, \theta_i, \psi_i\right) \begin{bmatrix} \hat{\mathbf{e}}_x \\ \hat{\mathbf{e}}_y \\ \hat{\mathbf{e}}_z \end{bmatrix}, \tag{26}$$

where

$$\mathbf{R}\left(\phi_i, \theta_i, \psi_i\right) = \begin{bmatrix} C_{\theta_i}C_{\psi_i} & C_{\theta_i}S_{\psi_i} & -S_{\theta_i} \\ S_{\phi_i}S_{\theta_i}C_{\psi_i} - C_{\phi_i}S_{\psi_i} & S_{\phi_i}S_{\theta_i}S_{\psi_i} + C_{\phi_i}C_{\psi_i} & S_{\phi_i}C_{\theta_i} \\ C_{\phi_i}S_{\theta_i}C_{\psi_i} + S_{\phi_i}S_{\psi_i} & C_{\phi_i}S_{\theta_i}S_{\psi_i} - S_{\phi_i}C_{\psi_i} & C_{\phi_i}C_{\theta_i} \end{bmatrix} \tag{27}$$

ϕ_i, θ_i, and ψ_i are the roll, pitch, and yaw angles of quadcopter $i \in \mathcal{V}$ relative to the inertial reference frame, $C_{(\cdot)}$ and $S_{(\cdot)}$ abbreviate "cos $(\cdot)$" and "sin $(\cdot)$", respectively.

Assumption 3. It is assumed that ψ_i is updated by the following dynamics:

$$\begin{cases} \psi_i[k+1] = \psi_i[k] + \Delta T\dot{\psi}_i[k] \\ \dot{\psi}_i[k+1] = \dot{\psi}_i[k], \end{cases} \tag{28}$$

subject to the initial conditions $\psi_i[0] = 0$ and $\dot{\psi}_i[0] = 0$ where time increment ΔT is constant at every discrete time k. Therefore, $\psi_i[k] = 0$ at every discrete time k.

The outer- and inner-loop dynamics of quadcopter $i \in \mathcal{V}$ are given by

$$\begin{bmatrix} \mathbf{r}_i[k+1] \\ \mathbf{v}_i[k+1] \\ \mathbf{a}_i[k+1] \\ \mathbf{J}_i[k+1] \end{bmatrix} = \begin{bmatrix} \mathbf{r}_i[k] + \Delta T\mathbf{v}_i[k] \\ \mathbf{v}_i[k] + \Delta T\mathbf{a}_i[k] \\ \mathbf{a}_i[k] + \Delta T\mathbf{J}_i[k] \\ \mathbf{J}_i[k] \end{bmatrix} + \Delta T \begin{bmatrix} \mathbf{0}_{9\times 3} \\ \mathbf{I}_3 \end{bmatrix} \mathbf{U}_i[k] \tag{29a}$$

$$\begin{bmatrix} \mathbf{\Lambda}_i[k+1] \\ \mathbf{\Gamma}_i[k+1] \\ \mathbf{\Xi}_i[k+1] \end{bmatrix} = \begin{bmatrix} \mathbf{\Lambda}_i[k] + \Delta T\mathbf{\Gamma}_i[k] \\ \mathbf{\Gamma}_i[k] + \Delta T\mathbf{\Xi}_i[k] \\ \mathbf{\Xi}_i[k] - \Delta T\mathbf{M}_i^{-1}\mathbf{H}_i \end{bmatrix} + \Delta T \begin{bmatrix} \mathbf{0}_{6\times 3} \\ m_i\mathbf{M}_i^{-1} \end{bmatrix} \mathbf{U}_i[k] \tag{29b}$$

where ΔT is time increment, $\mathbf{0}_{9\times 3}\in\mathbb{R}^{9\times 3}$ and $\mathbf{0}_{6\times 3}\in\mathbb{R}^{6\times 3}$ is the zero-entry matrices, $\mathbf{I}_3\in\mathbb{R}^{3\times 3}$ is the identity matrix, $\mathbf{\Lambda}_i[k]=[f_i[k]\ \phi_i[k]\ \theta_i[k]]^T$, $\mathbf{\Gamma}_i[k]=\left[\dot{f}_i[k]\ \dot{\phi}_i[k]\ \dot{\theta}_i[k]\right]^T$, and $\mathbf{\Xi}_i[k]=\left[\ddot{f}_i[k]\ \ddot{\phi}_i[k]\ \ddot{\theta}_i[k]\right]^T$. Matrices $\mathbf{M}_i=\mathbf{M}_i\left(f_i,\phi_i,\psi_i,\dot{f}_i,\dot{\phi}_i,\dot{\psi}_i\right)$ and $\mathbf{H}_i=\mathbf{H}_i\left(f_i,\phi_i,\psi_i,\dot{f}_i,\dot{\phi}_i,\dot{\psi}_i\right)$ are obtained in Appendix B. Note that $\mathbf{F}_i=f_i\hat{\mathbf{k}}_{b,i}$ is the thrust force generated by quadcopter i and f_i is the force magnitude.

Relation between inner-loop and outer-loop states: Using the Newton's Second law, acceleration of quadcopter i is obtained as follows:

$$\mathbf{a}_i[k]=-g\hat{\mathbf{e}}_z+\frac{f_i}{m_i}\hat{\mathbf{k}}_{b,i}[k], \tag{30}$$

$g=9.81m/s^2$ is the gravity. By taking derivatives from the acceleration of quadcopter i, the jerk and time derivative of the jerk are obtained as follows:

$$\mathbf{J}_i[k]=\frac{\dot{f}_i}{m_i}\hat{\mathbf{k}}_{b,i}+\frac{f_i}{m_i}\left(\vec{\omega}_i\times\hat{\mathbf{k}}_{b,i}\right), \tag{31a}$$

$$\mathbf{U}_i[k]=\frac{1}{m_i}\ddot{\mathbf{F}}_i=\frac{1}{m_i}\left(\mathbf{M}_i\mathbf{\Xi}_i+\mathbf{H}_i\right), \tag{31b}$$

where $\vec{\omega}_i$ is discussed in Appendix A and is the angular velocity of the quadcopter i with respect to the inertial reference frame and relationship (31b) is derived in Appendix B.

6. Quadcopter control

We choose control input

$$\mathbf{U}_i[k]=-\beta_1\mathbf{J}_i[k]-\beta_2\mathbf{a}_i[k]-\beta_3\mathbf{v}_i[k]+\beta_4\left(\mathbf{r}_{i,d}[k]-\mathbf{r}_i[k]\right) \tag{32}$$

where $\mathbf{r}_{i,d}$ is the local desired position of the vehicle $i\in\mathcal{V}$ and was previously defined in (6) and $\beta_1,\dots,\beta_4$ are constant control gains. The MQS coordination dynamics becomes

$$\mathbf{z}_{MQS}[k+1]=\mathbf{A}_{SYS}[k]\mathbf{z}_{MQS}[k]+\mathbf{B}_{SYS}[k]\mathbf{U}_{MQS}[k] \tag{33}$$

where

$$\mathbf{A}_{SYS}=$$

$$\mathbf{I}_3\otimes\left(\mathbf{I}_{4N}+\Delta T\begin{bmatrix}\mathbf{0}_N & \mathbf{I}_N & \mathbf{0}_N & \mathbf{0}_N\\ \mathbf{0}_N & \mathbf{0}_N & \mathbf{I}_N & \mathbf{0}_N\\ \mathbf{0}_N & \mathbf{0}_N & \mathbf{0}_N & \mathbf{I}_N\\ \beta_4\left(-\mathbf{I}_N+\mathbf{W}\right) & -\beta_3\mathbf{I}_N & -\beta_2\mathbf{I}_N & -\beta_1\mathbf{I}_N\end{bmatrix}\right),$$

$$\mathbf{B}_{SYS}=$$

$$\left(\mathbf{I}_3\otimes\left[\mathbf{0}_{(n+1)\times N}\ \ \mathbf{0}_{(n+1)\times N}\ \ \mathbf{0}_{(n+1)\times N}\ \ \Delta T\mathbf{I}_{n+1}\ \ \mathbf{0}_{(n+1)\times(N-n-1)}\right]\right)^T,$$

"$\otimes$" denotes the Kronecker product symbol, $\mathbf{0}_{n+1\times N}\in\mathbb{R}^{n+1\times N}$ and $\mathbf{0}_{n+1\times(N-n-1)}\in\mathbb{R}^{n+1\times(N-n-1)}$ are zero-entry matrices and $\mathbf{I}_3\in\mathbb{R}^{3\times 3}$, $\mathbf{I}_{n+1}\in\mathbb{R}^{n+1\times n+1}$, $\mathbf{I}_N\in\mathbb{R}^{N\times N}$ are identity matrices,

$$\mathbf{z}_{MQS}=\left[\mathbf{z}_x^T\ \cdots\ \dddot{\mathbf{z}}_x^T\ \ \mathbf{z}_y^T\ \cdots\ \dddot{\mathbf{z}}_y^T\ \ \mathbf{z}_z^T\ \cdots\ \dddot{\mathbf{z}}_z^T\right]^T\in\mathbb{R}^{12N\times 1}$$

is the quadcopter team state vector given by:

$$\mathbf{z}_x=[\mathbf{z}_{x,L}^T\ \mathbf{z}_{x,F}^T]^T,\ \mathbf{z}_{x,L}=[x_1\ \cdots\ x_{n+1}]^T,\ \mathbf{z}_{x,F}=[x_{n+2}\ \cdots\ x_N]^T,$$
$$\mathbf{z}_y=[\mathbf{z}_{y,L}^T\ \mathbf{z}_{y,F}^T]^T,\ \mathbf{z}_{y,L}=[y_1\ \cdots\ y_{n+1}]^T,\ \mathbf{z}_{y,F}=[y_{n+2}\ \cdots\ y_N]^T,$$
$$\mathbf{z}_z=[\mathbf{z}_{z,L}^T\ \mathbf{z}_{z,F}^T]^T,\ \mathbf{z}_{z,L}=[z_1\ \cdots\ z_{n+1}]^T,\ \mathbf{z}_{z,F}=[z_{n+2}\ \cdots\ z_N]^T.$$

Define a combined state for global positions of all vehicles in the network as

$$q\in\{x,y,z\},\qquad \mathbf{z}_{q,HT}[k]=\begin{bmatrix}\mathbf{z}_{q,HT,L}[k]\\ \mathbf{z}_{q,HT,F}[k]\end{bmatrix},$$

where

$$\mathbf{z}_{q,HT,L}=[q_{1,HT}\ \cdots\ q_{n+1,HT}]^T,$$
$$\mathbf{z}_{q,HT,F}=[q_{n+2,HT}\ \cdots\ q_{N,HT}]^T.$$

Control input $\mathbf{U}_{MQS}$ can be expressed as follows:

$$\mathbf{U}_{MQS}[k]=\beta_4\begin{bmatrix}\mathbf{z}_{x,HT,L}[k]\\ \mathbf{z}_{y,HT,L}[k]\\ \mathbf{z}_{z,HT,L}[k]\end{bmatrix} \tag{34}$$

Control gains $\beta_1,\dots,\beta_4$ are selected such that eigenvalues of matrix $\mathbf{A}_{SYS}$ are all placed inside a unit disk centered at the origin. Therefore, the BIBO[1] stability of the outerloop dynamics is ensured (see [31] for details).

Theorem 3. *Suppose graph $\mathcal{G}$ is defined such that Assumption 1 is satisfied and positive gains $\beta_1,\dots,\beta_4$ are selected such that eigenvalues of matrix $\mathbf{A}_{SYS}$ are inside an open unit disk centered at the origin. Then, the traffic network dynamics (33) is BIBO stable.*

Proof. It follows from Theorem 1 that if $\mathcal{G}$ is defined such that Assumption 1 is satisfied at every discrete time instant, then matrix $-\mathbf{I}_N+\mathbf{W}[k]$ has its eigenvalues inside the open unit ball centered at $-1+0j$. Given MQS collective dynamics (33), we can write

$$\mathbf{z}_{MQS}[k+1]=\mathbf{\Theta}_k\begin{bmatrix}\mathbf{z}_{MQS}[1]\\ \mathbf{B}_{SYS}[1]\mathbf{U}_{MQS}[1]\\ \vdots\\ \mathbf{B}_{SYS}[k]\mathbf{U}_{MQS}[k]\end{bmatrix}, \tag{35}$$

where

$$\mathbf{\Theta}_k=\left[\mathbf{\Gamma}_k\ \ \cdots\ \ \mathbf{\Gamma}_1\ \ \mathbf{\Gamma}_0\right] \tag{36a}$$

$$\mathbf{\Gamma}_h=\prod_{j=k-h+1}^{k}\mathbf{A}_{SYS}[j] \tag{36b}$$

for $h=1,\cdots,k$, and $\mathbf{\Gamma}_0=\mathbf{I}_{12N}$ is an identity matrix. Since $\mathbf{z}_{MQS}[1]$ is bounded as the network system's initial condition and $\mathbf{U}_{MQS}[k]$ is bounded at every discrete time k, there exists a constant $z_{max}>0$ such that

$$\mathbf{z}_{MQS}[1]\le z_{max}\mathbf{1}_{12N\times 1}, \tag{37a}$$

$$|\mathbf{B}_{SYS}[k]\mathbf{u}_{MQS}[k]|\le z_{max}\mathbf{1}_{12N\times 1}, \tag{37b}$$

where $\mathbf{1}_{12N\times 1}\in\mathbb{R}^{12N}$ is the vector ones and the notation $|x|$ in (37b) denotes a vector composed of absolute values of the entries of x. If assumptions of Theorem 3 are satisfied, spectral radius of matrix $\mathbf{\Gamma}_k$ is less than $r<1$ at every discrete time k. Therefore, we can write

$$\begin{aligned}&\mathbf{z}_{MQS}^T[k+1]\mathbf{z}_{MQS}[k+1]\\ &\le z_{max}\mathbf{1}_{12N\times 1}^T\left(\sum_{l=0}^{k}\sum_{h=0}^{k}\mathbf{\Gamma}_l^T\mathbf{\Gamma}_h\right)z_{max}\mathbf{1}_{12N\times 1}\\ &\le 12Nz_{max}^2\left(\sum_{l=0}^{\infty}r^l\right)\le\frac{12Nz_{max}^2}{(1-r)}.\end{aligned} \tag{38}$$

This implies that $\mathbf{z}_{MQS}^T[k+1]\mathbf{z}_{MQS}[k+1]$ is bounded at every discrete time k, and thus the BIBO stability of traffic dynamics (33) is proven. □

[1] BIBO stands for Bounded Input Bounded Output.

Remark 2. It follows from the proof of Theorem 3 that the convergence of the state $\mathbf{z}_{\text{MQS}}[k]$ to its desired value as $k \to \infty$ can be ensured under the condition that $\mathbf{u}_{\text{MQS}}[k] \to 0$ as $k \to \infty$ which means that the convergent input implies convergent state.

Assumption 4. It is assumed that every quadcopter $i \in \mathcal{V}$ is able to choose an admissible control input $\mathbf{U}_i[k]$ at discrete time k such that

$$\forall i \in \mathcal{V}, \forall k,\ q \in \{x, y, z\}, \qquad \left|q_i[k] - q_{i,HT}[k]\right| \le \delta - \epsilon. \tag{39}$$

Then, safety constraint (9) is satisfied at every discrete time k which in turn implies that quadcopter i never leaves the safety box $\mathcal{B}_i$ centered at $\mathbf{r}_{i,HT}[k]$ at discrete time k.

Remark 3. Let

$$\mathbf{y}_{q,HT}[k] = \begin{bmatrix} \mathbf{z}^T_{q,L,HT}[k] & \mathbf{z}^T_{q,F,HT}[k] \end{bmatrix}^T \in \mathbb{R}^{N\times 1}, \qquad q \in \{x, y, z\}, \tag{40a}$$

$$\mathbf{y}_{q,d}[k] = \begin{bmatrix} q_{1,d}[k] & \cdots & q_{N,d}[k] \end{bmatrix}^T \in \mathbb{R}^{N\times 1}, \qquad q \in \{x, y, z\}, \tag{40b}$$

$$\mathbf{y}_{q}[k] = \begin{bmatrix} q_{1}[k] & \cdots & q_{N}[k] \end{bmatrix}^T \in \mathbb{R}^{N\times 1}, \qquad q \in \{x, y, z\} \tag{40c}$$

be an aggregate component $q \in \{x, y, z\}$ of the quadcopters' global desired positions, local desired positions, and actual positions, respectively. Then, it was shown in [32] that $\mathbf{y}_{q,HT}[k]$, $\mathbf{y}_{q,d}[k]$, and $\mathbf{y}_q[k]$ are related as

$$\mathbf{Y}_{q,d}[k] - \mathbf{Y}_q[k] = \mathbf{D}\left(\mathbf{Y}_{q,HT}[k] - \mathbf{Y}_d[k]\right). \tag{41}$$

Therefore, there exists a $\zeta_i > 0$ such that

$$\left|q_i[k] - q_{i,d}[k]\right| < \zeta_i \implies \left|q_i[k] - q_{i,HT}[k]\right| \le \delta - \epsilon,$$
$$\forall i \in \mathcal{V},\ q \in \{x, y, z\},\ \forall k.$$

Hence, safety condition (39) is satisfied, if the leaders' desired trajectories are planned such that each quadcopter $i \in \mathcal{V}$ can track the local desired trajectory $\mathbf{r}_{i,d}$ and $\left|q_i[k] - q_{i,d}[k]\right| < \zeta_i$ at every discrete time k.

7. Safety specification

The MQS continuum deformation is labeled “safe” if constraints (9), (11) and (13) are all satisfied for every quadcopter $i \in \mathcal{V}$. Per Assumption 4, every quadcopter $i \in \mathcal{V}$ is able to ensure that the safety constraint (9) is satisfied at every discrete time k. The following theorem ensures the satisfaction of the safety requirements (11) and (13) by imposing constraints on the time-varying communication weights of followers as well as the global desired trajectories of the leaders.

Theorem 4. *Assume quadcopter i chooses the control input* $\mathbf{U}_i$ *such that safety constraint* (9) *is satisfied at every discrete time k. Let graph* $\mathcal{G}$ *be connected and planar and in-neighbors of follower* $i \in \mathcal{V}_F$ *are defined by set* $\mathcal{N}_i = \{i_1, \cdots, i_{n+1}\}$. *Inter-agent collision avoidance (safety condition* (11)*) and follower containment condition (safety condition* (13)*) are guaranteed, if followers' communication weights satisfy the following inequality and equality constraints:*

$$\forall k,\ \forall i_j \in \mathcal{N}_i,\ \forall i \in \mathcal{V}_F, \qquad w_{i,i_j}[k] \ge 0, \tag{42a}$$

$$\forall k, \forall i \in \mathcal{V}_F, \qquad \sum_{j=1}^{n+1} w_{i,i_j}[k] = 1, \tag{42b}$$

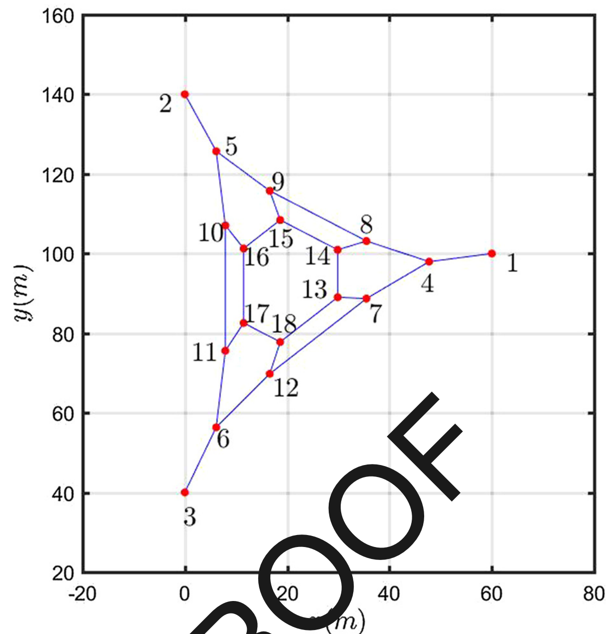

Fig. 1. MQS initial formation and the communication graph used by followers to acquire the desired affine transformation.

$$\forall k, \quad \bigwedge_{q\in\{x,y,z\}} \bigwedge_{\forall i\in\mathcal{V}_F} \bigwedge_{\forall j\in\mathcal{N}_i} \left(\left| \sum_{l=1}^{n+1} \left(\alpha_{i,L} - \alpha_{j,L}\right) q_{L,HT}[k] \right| \ge 2\epsilon \right), \tag{42c}$$

$$\forall k, \quad \bigwedge_{i\in\mathcal{V}_F} \underbrace{\bigwedge_{j_1=1}^{8} \cdots \bigwedge_{j_{n+1}=1}^{8}}_{\text{n+1 } times} \times \bigwedge_{(\mathbf{b}_{i_1,j}[k],\cdots,\mathbf{b}_{i_{n+1},j}[k])\in\mathcal{S}} \rho\left(\mathbf{b}_{i_1,j_1}[k], \cdots, \mathbf{b}_{i_{n+1},j_{n+1}}[k]\right) = n, \tag{42d}$$

$$\forall k, \quad \bigwedge_{i\in\mathcal{V}_F} \underbrace{\bigwedge_{j_1=1}^{8} \cdots \bigwedge_{j_{n+1}=1}^{8}}_{\text{n+1 } times} \bigwedge_{\left(\mathbf{b}_{i_1,j}[k],\cdots,\mathbf{b}_{i_{n+1},j}[k]\right)\in\mathcal{S}} \times \boldsymbol{\Omega}\left(\mathbf{b}_{i_1,j_1}[k], \cdots, \mathbf{b}_{i_{n+1},j_{n+1}}[k], \mathbf{r}_i[k]\right) \ge 0 \tag{42e}$$

,

Proof. If communication graph $\mathcal{G}$ is connected and planar and communication weights are chosen such that (42a) and (42b) are satisfied, then global desired position of follower $i \in \mathcal{V}_F$ is inside the simplex made by the global desired positions of the in-neighbors of $i \in \mathcal{V}_F$. If condition (42c) is satisfied, quadcopter $i \in \mathcal{V}_F$ does not collide with its in-neighbors. The polytope made by actual positions of in-neighbors of follower $i \in \mathcal{V}_F$ in an n-D simplex, if safety condition (42d) is satisfied. Furthermore, follower i does not leave the simplex made by actual positions of the in-neighbors of follower $i \in \mathcal{V}_F$, if (42e) is satisfied. Therefore, no two quadcopters collide and no quadcopter leaves the leading simplex defined by leaders if follower communication weights satisfy the safety condition (42a) through (42e) at every discrete time k. □

8. Simulation results

We consider an MQS consisting of 18 quadcopters with the initial formation shown in Fig. 1. Quadcopters are classified as lead-

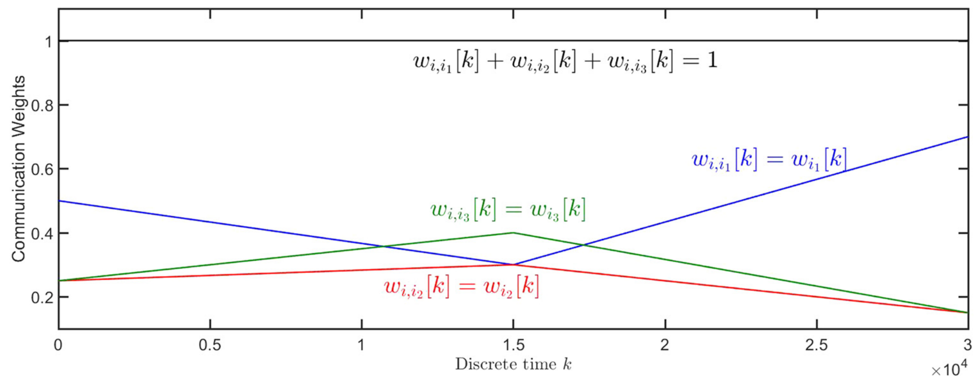

Fig. 2. Followers' communication weight versus discrete time k.

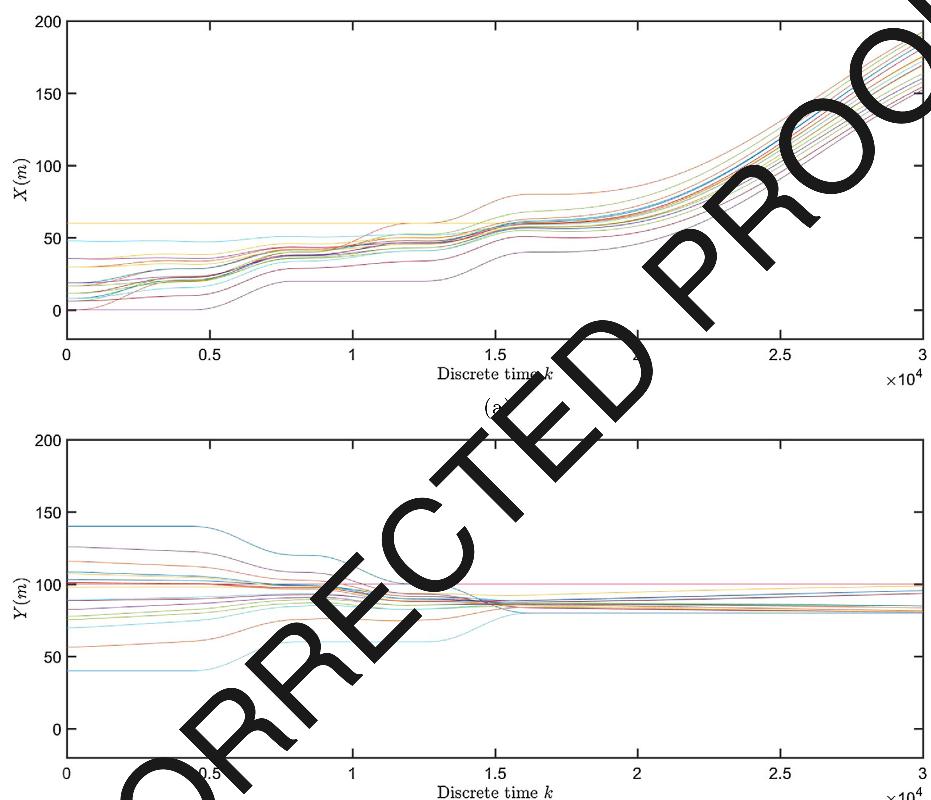

(b)

Fig. 3. MQS formations at (a) $k=5000$, (b) $k=10000$, (c) $k=20000$, (d) $k=25000$ and (e) $k=30000$.

ers and followers where leaders and followers are defined by sets $\mathcal{V}_L=\{1,2,3\}$ and $\mathcal{V}_F=\{4,\cdots,18\}$, respectively. The MQS applies the communication graph shown in Fig. 1 to acquire the desired continuum deformation through local communication. For every follower quadcopter i, the in-neighbor set is unchanged and is listed in Table below. In Fig. 2, followers' communication weights are plotted versus time. Given communication weights, leaders move independently and followers acquire the desired continuum deformation via local communication. In Figs. 3 (a) and (b), x and y components of actual positions of all quadcopters are plotted versus time. Furthermore, MQS formation at discrete times $k=5000$, $k=10000$, $k=15000$, $k=25000$, and $k=30000$ are illustrated in Figs. 4 (a-e).

$i\in\mathcal{V}_F$	$\mathcal{N}_i$		
	i_1	i_2	i_3
4	1	7	8
5	2	9	10
6	3	11	12
7	4	12	13
8	4	9	14
9	5	8	15
10	5	11	16
11	6	10	17
12	6	7	18
13	7	14	18
14	8	13	15
15	9	14	16
16	10	15	17
17	11	16	18
18	12	13	17

9. Conclusion

This paper studied the problem of continuum deformation of a MQS under time-varying communication weights. We showed how quadcopters can be treated as particles of a continuum (deformable body) with time-varying properties while stability, con-

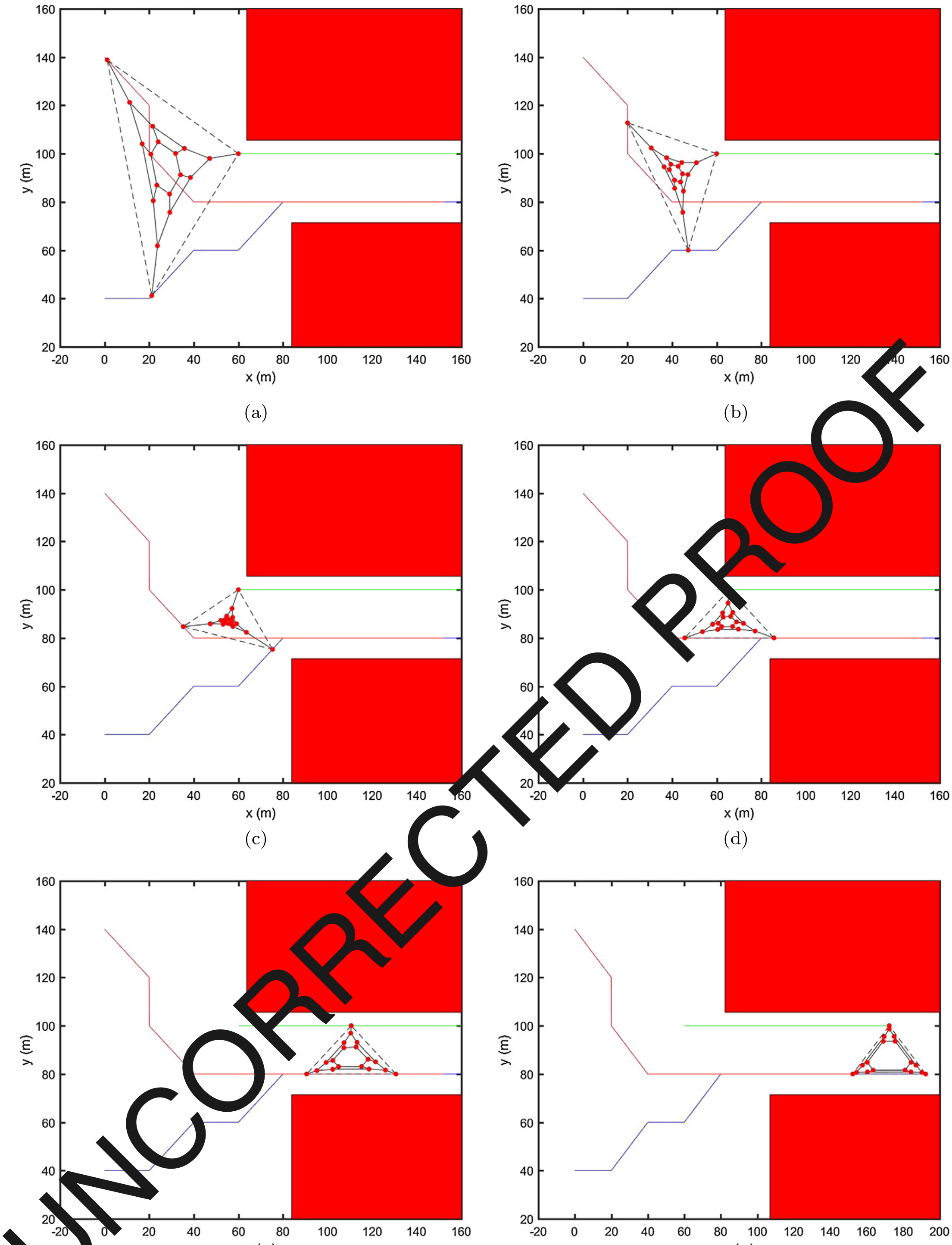

Fig. 4. MQS formations at (a) $k = 5000$, (b) $k = 10000$, (c) $k = 20000$, (d) $k = 25000$ and (e) $k = 30000$.

vergence, and containment of the group coordination, defined by a continuum deformation, can be guaranteed. By formal specification of the safety requirements, the scalability of collective motion can be significantly improved while the MQS can aggressively deform in a geometrically-constrained environment. Furthermore, this paper advances maneuverability of the collective motion via choosing time-varying communication weights. As a future work, we plan to advance the proposed MQS continuum deformation coordination under time-varying communication weights towards MQS continuum deformation under time-varying communication protocol in which communication weights and links can vary with time. In particular, we plan to formally specify and verify safety of the MQS coordination in an obstacle-laden motion space.

Declaration of competing interest

The authors certify that they have NO affiliations with or involvement in any organization or entity with any financial interest (such as honoraria; educational grants; participation in speakers' bureaus; membership, employment, consultancies, stock ownership, or other equity interest; and expert testimony or patent-licensing arrangements), or non-financial interest (such as personal or professional relationships, affiliations, knowledge or beliefs) in the subject matter or materials discussed in this manuscript.

Acknowledgement

The author gratefully thanks Professor Anthony Waas and Professor Veera Sundararaghavan for useful discussions.

Appendix A. Quadcopter angular velocity and acceleration

We use 3-2-1 standard Euler angle rotations to determine orientation of quadcopter i at discrete time k. Given roll angle $\phi_i[k]$, pitch angle θ_i, and yaw angle ψ_i and the base vectors of the inertial coordinate system ($\hat{\mathbf{e}}_x$, $\hat{\mathbf{e}}_y$, and $\hat{\mathbf{e}}_z$), angular velocity of quadcopter $i \in \mathcal{V}$ is given by

$$\vec{\omega}_i = \dot{\psi}_i \hat{\mathbf{k}}_{1,i} + \dot{\theta}_i \hat{\mathbf{j}}_{2,i} + \dot{\phi}_i \hat{\mathbf{i}}_{b,i}, \tag{A.1}$$

where

$$\begin{bmatrix} \hat{\mathbf{i}}_{1,i} \\ \hat{\mathbf{j}}_{1,i} \\ \hat{\mathbf{k}}_{1,i} \end{bmatrix} = \mathbf{R}(0,0,\psi_i) \begin{bmatrix} \hat{\mathbf{e}}_x \\ \hat{\mathbf{e}}_y \\ \hat{\mathbf{e}}_z \end{bmatrix} = \begin{bmatrix} \cos\psi_i & \sin\psi_i & 0 \\ -\sin\psi_i & \cos\psi_i & 0 \\ 0 & 0 & 1 \end{bmatrix} \begin{bmatrix} \hat{\mathbf{e}}_x \\ \hat{\mathbf{e}}_y \\ \hat{\mathbf{e}}_z \end{bmatrix}, \tag{A.2a}$$

$$\begin{bmatrix} \hat{\mathbf{i}}_{2,i} \\ \hat{\mathbf{j}}_{2,i} \\ \hat{\mathbf{k}}_{2,i} \end{bmatrix} = \mathbf{R}(0,\theta_i,0) \begin{bmatrix} \hat{\mathbf{i}}_{1,i} \\ \hat{\mathbf{j}}_{1,i} \\ \hat{\mathbf{k}}_{1,i} \end{bmatrix} = \begin{bmatrix} \cos\theta_i & 0 & -\sin\theta_i \\ 0 & 1 & 0 \\ \sin\theta_i & 0 & \cos\theta_i \end{bmatrix} \begin{bmatrix} \hat{\mathbf{i}}_{1,i} \\ \hat{\mathbf{j}}_{1,i} \\ \hat{\mathbf{k}}_{1,i} \end{bmatrix}, \tag{A.2b}$$

$$\begin{bmatrix} \hat{\mathbf{i}}_{b,i} \\ \hat{\mathbf{j}}_{b,i} \\ \hat{\mathbf{k}}_{b,i} \end{bmatrix} = \mathbf{R}(\phi_i,0,0) \begin{bmatrix} \hat{\mathbf{i}}_{2,i} \\ \hat{\mathbf{j}}_{2,i} \\ \hat{\mathbf{k}}_{2,i} \end{bmatrix} = \begin{bmatrix} 1 & 0 & 0 \\ 0 & \cos\phi_i & \sin\phi_i \\ 0 & -\sin\phi_i & \cos\phi_i \end{bmatrix} \begin{bmatrix} \hat{\mathbf{i}}_{2,i} \\ \hat{\mathbf{j}}_{2,i} \\ \hat{\mathbf{k}}_{2,i} \end{bmatrix}. \tag{A.2c}$$

Fig. A.5 shows the schematic of the inertial coordinate system with base vectors $\hat{\mathbf{e}}_x$, $\hat{\mathbf{e}}_y$, and $\hat{\mathbf{e}}_z$ and the body frame of quadcopter $i \in \mathcal{V}$ with base vectors $\hat{\mathbf{i}}_{b,i}$, $\hat{\mathbf{j}}_{b,i}$, and $\hat{\mathbf{k}}_{b,i}$. Substituting $\hat{\mathbf{e}}_x = [1\ 0\ 0]^T$, $\hat{\mathbf{e}}_y = [0\ 1\ 0]^T$, $\hat{\mathbf{e}}_z = [0\ 0\ 1]^T$, $\hat{\mathbf{i}}_{1,i}$, $\hat{\mathbf{k}}_{1,i}$, $\hat{\mathbf{j}}_{2,i}$, and $\hat{\mathbf{i}}_{b,i}$ into Eq. (A.1), $\vec{\omega}_i = \left[\omega_{x,i}\ \omega_{y,i}\ \omega_{z,i}\right]^T$ resolved in the body frame is related to $\dot{\phi}_i$, $\dot{\theta}_i$, and $\dot{\psi}_i$ by

$$\begin{bmatrix} \omega_{x,i} \\ \omega_{y,i} \\ \omega_{z,i} \end{bmatrix} = \begin{bmatrix} 1 & 0 & -\sin\theta_i \\ 0 & \cos\phi_i & \cos\theta_i \sin\phi_i \\ 0 & -\sin\phi_i & \cos\phi_i \cos\theta_i \end{bmatrix} \begin{bmatrix} \dot{\phi}_i \\ \dot{\theta}_i \\ \dot{\psi}_i \end{bmatrix}. \tag{A.3}$$

Angular acceleration of quadcopter $i \in \mathcal{V}$ is obtained by taking time derivative of the angular velocity vector $\vec{\omega}_i$ with respect to the inertial reference frame:

$$\begin{aligned} \dot{\vec{\omega}} =& \ddot{\psi}_i \hat{\mathbf{k}}_{1,i} + \ddot{\theta}_i \hat{\mathbf{j}}_{2,i} + \ddot{\phi}_i \hat{\mathbf{i}}_{b,i} + \dot{\theta}_i \dot{\psi}_i \left(\hat{\mathbf{k}}_{1,i} \times \hat{\mathbf{j}}_{1,i} \right) \\ &+ \dot{\phi}_i \left(\dot{\psi}_i \hat{\mathbf{k}}_{1,i} + \dot{\theta}_i \hat{\mathbf{j}}_{2,i} \right) \times \hat{\mathbf{i}}_{2,i} \end{aligned} \tag{A.4}$$

Remark 4. Per Assumption 3, $\psi_i[k] = 0$ at every discrete time $k \in \mathbb{Z}$. Therefore, $\hat{\mathbf{i}}_{1,i} = \hat{\mathbf{e}}_x = [1\ 0\ 0]^T$, $\hat{\mathbf{j}}_{1,i} = \hat{\mathbf{e}}_y = [0\ 1\ 0]^T$, $\hat{\mathbf{k}}_{1,i} = \hat{\mathbf{e}}_z = [0\ 0\ 1]^T$, and $\vec{\omega}_i$ and $\dot{\vec{\omega}}_i$ simplify to

$$\vec{\omega}_i = \dot{\theta}_i \hat{\mathbf{j}}_{2,i} + \dot{\phi}_i \hat{\mathbf{i}}_{b,i}, \tag{A.5a}$$

$$\dot{\vec{\omega}} = \ddot{\theta}_i \hat{\mathbf{j}}_{2,i} + \ddot{\phi}_i \hat{\mathbf{i}}_{b,i} - \dot{\phi}_i \dot{\theta}_i \hat{\mathbf{k}}_{2,i}. \tag{A.5b}$$

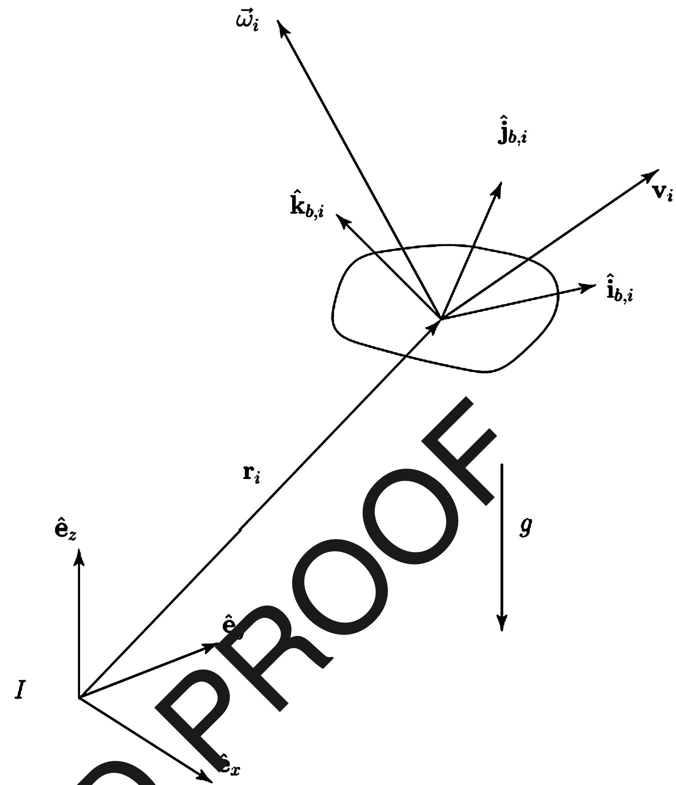

Fig. A.5. Schematic of the inertial coordinate system fixed on the ground and the body frame of quadcopter $i \in \mathcal{V}$.

Appendix B. Time derivatives of the quadcopter thrust force

Taking time derivatives from the quadcopter thrust force $\mathbf{F}_i = m_i \mathbf{a}_i = f_i \hat{\mathbf{k}}_{b,i}$, we obtain the following relations:

$$\dot{\mathbf{F}}_i = \dot{f}_i \hat{\mathbf{k}}_{b,i} + f_i \vec{\omega}_i \times \hat{\mathbf{k}}_{b,i} \tag{B.1a}$$

$$\ddot{\mathbf{F}}_i = \ddot{f}_i \hat{\mathbf{k}}_{b,i} + f_i \left[\dot{\vec{\omega}}_i \times \hat{\mathbf{k}}_{b,i} + \vec{\omega}_i \times \left(\vec{\omega}_i \times \hat{\mathbf{k}}_{b,i} \right) \right] + 2 \dot{f}_i \vec{\omega}_i \times \hat{\mathbf{k}}_{b,i} \tag{B.1b}$$

By rearranging Eq. (B.1b), $\ddot{\mathbf{F}}_i$ is expressed as follows:

$$\ddot{\mathbf{F}}_i = \mathbf{M}_i \Xi_i + \mathbf{H}_i, \tag{B.2}$$

where $\Xi_i = \left[\ddot{f}_i \quad \ddot{\phi}_i \quad \ddot{\theta}_i \right]^T$,

$$\mathbf{M}_i = \left[\hat{\mathbf{k}}_{b,i} \,\middle|\, -f_i \hat{\mathbf{j}}_{b,i} \,\middle|\, f_i \left(\hat{\mathbf{j}}_{2,i} \times \hat{\mathbf{k}}_{b,i} \right) \right] \in \mathbb{R}^{3\times 3}, \tag{B.3a}$$

$$\mathbf{H}_i = f_i \left[-\dot{\phi}_i \dot{\theta}_i \left(\hat{\mathbf{k}}_{2,i} \times \hat{\mathbf{k}}_{b,i} \right) + \vec{\omega}_i \times \left(\vec{\omega}_i \times \hat{\mathbf{k}}_{b,i} \right) \right] + 2 \dot{f}_i \vec{\omega}_i \times \hat{\mathbf{k}}_{b,i}. \tag{B.3b}$$

Remark 5. In equations of Appendix B, $\hat{\mathbf{k}}_{b,i}$, $\hat{\mathbf{j}}_{b,i}$, $\hat{\mathbf{j}}_{2,i}$, and $\hat{\mathbf{k}}_{2,i}$ are 3 by 1 unit vectors expressed with respect to the initial coordinate system with base vectors $\hat{\mathbf{e}}_x$, $\hat{\mathbf{e}}_y$, $\hat{\mathbf{e}}_z$.

References

[1] S.-L. Du, X.-M. Sun, M. Cao, W. Wang, Pursuing an evader through cooperative relaying in multi-agent surveillance networks, Automatica 83 (2017) 155–161.
[2] L.C.B. da Silva, R.M. Bernardo, H.A. de Oliveira, P.F. Rosa, Multi-UAV agent-based coordination for persistent surveillance with dynamic priorities, in: 2017 International Conference on Military Technologies, ICMT, IEEE, 2017, pp. 765–771.
[3] E. Rojo-Rodriguez, E. Ollervides, J. Rodriguez, E. Espinoza, P. Zambrano-Robledo, O. Garcia, Implementation of a super twisting controller for distributed formation flight of multi-agent systems based on consensus algorithms, in: 2017 International Conference on Unmanned Aircraft Systems, ICUAS, IEEE, 2017, pp. 1101–1107.

[4] S.-h. Ha, S.-d. Chi, Multi-agent based design of autonomous UAVs for both flocking and formation flight, J. Adv. Navig. Technol. 21 (6) (2017) 521–528.

[5] M. Xu, K. An, L.H. Vu, Z. Ye, J. Feng, E. Chen, Optimizing multi-agent based urban traffic signal control system, J. Intell. Transp. Syst. 23 (4) (2019) 357–369.

[6] H. AlTair, T. Taha, J. Dias, M. Al-Qutayri, Decision making for multi-objective multi-agent search and rescue missions, in: 2017 International Conference on Electrical and Computing Technologies and Applications, ICECTA, IEEE, 2017, pp. 1–4.

[7] H. Rastgoftar, E.M. Atkins, Cooperative aerial lift and manipulation (calm), Aerosp. Sci. Technol. 82 (2018) 105–118.

[8] F. Rossomando, C. Rosales, J. Gimenez, L. Salinas, C. Soria, M. Sarcinelli-Filho, R. Carelli, Aerial load transportation with multiple quadrotors based on a kinematic controller and a neural SMC dynamic compensation, J. Intell. Robot. Syst. 100 (2) (2020) 519–530.

[9] L. Dong, Y. Chen, X. Qu, Formation control strategy for nonholonomic intelligent vehicles based on virtual structure and consensus approach, Proc. Eng. 137 (2016) 415–424.

[10] D. Zhang, Z. Xu, D. Srinivasan, L. Yu, Leader–follower consensus of multiagent systems with energy constraints: a Markovian system approach, IEEE Trans. Syst. Man Cybern. Syst. 47 (7) (2017) 1727–1736.

[11] W. Liu, S. Zhou, Y. Qi, X. Wu, Leaderless consensus of multi-agent systems with Lipschitz nonlinear dynamics and switching topologies, Neurocomputing 173 (2016) 1322–1329.

[12] Z. Zhen, G. Tao, Y. Xu, G. Song, Multivariable adaptive control based consensus flight control system for UAVs formation, Aerosp. Sci. Technol. 93 (2019) 105336.

[13] H. Gui, G. Vukovich, Distributed almost global finite-time attitude consensus of multiple spacecraft without velocity measurements, Aerosp. Sci. Technol. 75 (2018) 284–296.

[14] F. Sun, Y. Shen, J. Kurths, W. Zhu, Mean-square consensus of multi-agent systems with noise and time delay via event-triggered control, J. Franklin Inst. 357 (9) (2020) 5317–5339.

[15] Q. Ma, J. Qin, W.X. Zheng, Y. Shi, Y. Kang, Exponential consensus of linear systems over switching network: a subspace method to establish necessity and sufficiency, IEEE Trans. Cybern..

[16] C. Wang, Z. Ding, H_∞ consensus control of multi-agent systems with input delay and directed topology, IET Control Theory Appl. 10 (6) (2016) 617–624.

[17] Y. Cao, W. Ren, M. Egerstedt, Distributed containment control with multiple stationary or dynamic leaders in fixed and switching directed networks, Automatica 48 (8) (2012) 1586–1597.

[18] M. Ji, G. Ferrari-Trecate, M. Egerstedt, A. Buffa, Containment control in mobile networks, IEEE Trans. Autom. Control 53 (8) (2008) 1972–1975.

[19] S. Xingling, T. Biao, Y. Wei, Z. Wendong, Estimator-based MLP neuroadaptive dynamic surface containment control with prescribed performance for multiple quadrotors, Aerosp. Sci. Technol. (2019) 105620.

[20] D. Wang, W. Wang, Necessary and sufficient conditions for containment control of multi-agent systems with time delay, Automatica 103 (2019) 418–423.

[21] Z. Li, T. Li, R. Yuan, S. Fei, Further results on containment control for multi-agent systems with variable communication delay, Arab. J. Sci. Eng. 44 (3) (2019) 2665–2677.

[22] J. Shen, J. Lam, Containment control of multi-agent systems with unbounded communication delays, Int. J. Syst. Sci. 47 (9) (2016) 2048–2057.

[23] C. Ding, X. Dong, C. Shi, Y. Chen, Z. Liu, Leaderless output consensus of multi-agent systems with distinct relative degrees under switching directed topologies, IET Control Theory Appl. 13 (3) (2018) 313–320.

[24] B. Tian, H. Lu, Z. Zuo, W. Yang, Fixed-time leader–follower output feedback consensus for second-order multiagent systems, IEEE Trans. Cybern. 49 (4) (2018) 1545–1550.

[25] B. Li, Z.-Q. Chen, C.-Y. Zhang, Z.-X. Liu, Q. Zhang, Containment control for directed networks multi-agent system with nonlinear dynamics and communication time-delays, Int. J. Control. Autom. Syst. 15 (3) (2017) 1181–1188.

[26] H. Lü, W. He, Q.-L. Han, X. Ge, C. Peng, Finite-time containment control of nonlinear multi-agent systems with non-singular terminal sliding mode, in: 2018 Australian & New Zealand Control Conference, ANZCC, IEEE, 2018, pp. 222–226.

[27] Z. Yu, Z. Liu, Y. Zhang, Y. Qu, C.-Y. Su, Distributed finite-time fault-tolerant containment control for multiple unmanned aerial vehicles, IEEE Trans. Neural Netw. Learn. Syst. 31 (6) (2020) 2077–2091.

[28] H. Rastgoftar, Continuum deformation of a multi-agent system over nonlinear surfaces, in: Continuum Deformation of Multi-Agent Systems, Springer, 2016, pp. 185–194.

[29] Z. Qu, Cooperative Control of Dynamical Systems: Applications to Autonomous Vehicles, Springer Science & Business Media, 2009.

[30] X. Liu, H. Rastgoftar, Conservation-based modeling and boundary control of congestion with an application to traffic management in center city Philadelphia, arXiv preprint, arXiv:2102.00552.

[31] H. Rastgoftar, E. Atkins, An integrative data-driven physics-inspired approach to traffic congestion control, arXiv preprint, arXiv:1912.00565.

[32] H. Rastgoftar, Fault-resilient continuum deformation coordination, IEEE Trans. Control Netw. Syst. 8 (1) (2021) 423–436.